nature neuroscience

Dynorphin A activates bradykinin receptors to maintain neuropathic pain

Josephine Lai, Miaw-Chyi Luo, Qingmin Chen, Shouwu Ma, Luis R Gardell, Michael H Ossipov & Frank Porreca

Dynorphin A is an endogenous opioid peptide that produces non-opioid receptor-mediated neural excitation. Here we demonstrate that dynorphin induces calcium influx via voltage-sensitive calcium channels in sensory neurons by activating bradykinin receptors. This action of dynorphin at bradykinin receptors is distinct from the primary signaling pathway activated by bradykinin and underlies the hyperalgesia produced by pharmacological administration of dynorphin by the spinal route in rats and mice. Blockade of spinal B1 or B2 receptor also reverses persistent neuropathic pain but only when there is sustained elevation of endogenous spinal dynorphin, which is required for maintenance of neuropathic pain. These data reveal a mechanism for endogenous dynorphin to promote pain through its agonist action at bradykinin receptors and suggest new avenues for therapeutic intervention.

Opioid receptors and their endogenous peptide ligands regulate pain, a variety of autonomic and motor functions and responses to stress[1]. Opioid peptides include enkephalins, endorphins and dynorphins. Dynorphin $A_{1–17}$, a major proteolytic fragment of prodynorphin[2,3], exhibits high affinity for μ, δ and κ opioid receptors[4–6]. However, the role of dynorphin A in antinociception remains unclear. In the spinal cord, dynorphin has both inhibitory effects mediated by opioid receptors and excitatory effects mediated through an unknown mechanism. Intrathecal dynorphin A produces only modest antinociceptive effects[7] as well as prominent excitatory effects, which include abnormal pain and severe motor dysfunction[8–11]. Spinal dynorphin stimulates the release of excitatory amino acids and prostaglandin E_2 (ref. 12). Dynorphin A stimulates the release of excitatory amino acids from cultured neurons[13], induces an increase in intracellular calcium[14] and may be excitotoxic at high doses[15]. The mechanisms of these excitatory actions of dynorphin are unknown but do not involve actions at opioid receptors.

Many experimental models of chronic pain[16–19] show significant and time-dependent regional elevation of dynorphin A in the spinal cord. Intrathecal administration of an anti-dynorphin A antiserum blocks pain induced by peripheral nerve injury[17,20] and opioid-induced hyperalgesia[19], suggesting that the elevated level of spinal dynorphin in these models is necessary for maintaining chronic pain. Nerve injury produces abnormal pain in transgenic mice with a null mutation in the prodynorphin gene, but such pain is not maintained, indicating a requirement for elevation of spinal dynorphin in persistent neuropathic pain[20]. Here we report that bradykinin receptors mediate the excitatory actions of dynorphin on sensory neurons and underlie the pronociceptive effects of spinal dynorphin.

RESULTS

Dynorphin A activates VSCCs to raise intracellular calcium

A hybridoma of embryonic rat dorsal root ganglion (DRG) cells and mouse neuroblastoma cells called F-11 (ref. 21) was used as a cell model of peripheral sensory neurons to characterize the effects of dynorphin A. F-11 cells retain a number of characteristics of sensory neurons, including the expression of the excitatory neuropeptide substance P (refs. 21,22), receptors for bradykinin and prostaglandin[22], μ and δ opioid receptors[23] and responsiveness to nerve growth factor[22]. They also showed a rapidly desensitizing response to capsaicin characteristic of nociceptive C fibers due to the expression of vanilloid receptor type I (**Supplementary Fig. 1** online). These cells also expressed voltage sensitive calcium channels (VSCCs), including N, L, T and P/Q type[22] (**Supplementary Fig. 2** online). To evaluate selectively the non-opioid receptor-mediated effects of dynorphin A, we used a des-tyrosyl fragment of dynorphin A, dynorphin $A_{2–13}$, which had very low affinity for all three opioid receptor types (**Supplementary Fig. 3** online). F-11 cells also lacked specific binding of the kappa receptor-selective agonist, [^{3}H]U69,593. Ratiometric fura-2 fluorescence imaging of intracellular calcium concentration ($[Ca^{2+}]_i$) showed that dynorphin $A_{2–13}$ consistently induced a transient increase in $[Ca^{2+}]_i$ in a dose-dependent manner in primary cultures of embryonic DRG (**Fig. 1a**) and in F-11 cells (**Fig. 1b**). The minimum effective concentration of dynorphin $A_{2–13}$ was 500 nM. At 5 μM dynorphin $A_{2–13}$, 67% of the total recorded cells (663 of 994) showed an increase in $[Ca^{2+}]_i$. The response to dynorphin A was observed only in cells that responded to a depolarizing concentration of KCl ($n = 663$). The opioid receptor antagonist, naloxone (1 μM) had no effect on the response to dynorphin $A_{2–13}$ ($n = 81$). The opioid peptide dynorphin

Department of Pharmacology, University of Arizona Health Sciences Center, 1501 N. Campbell Ave., Tucson, Arizona 85724, USA. Correspondence should be addressed to J.L. (lai@u.arizona.edu).

Received 19 September; accepted 25 October; published online 19 November 2006; doi:10.1038/nn1804

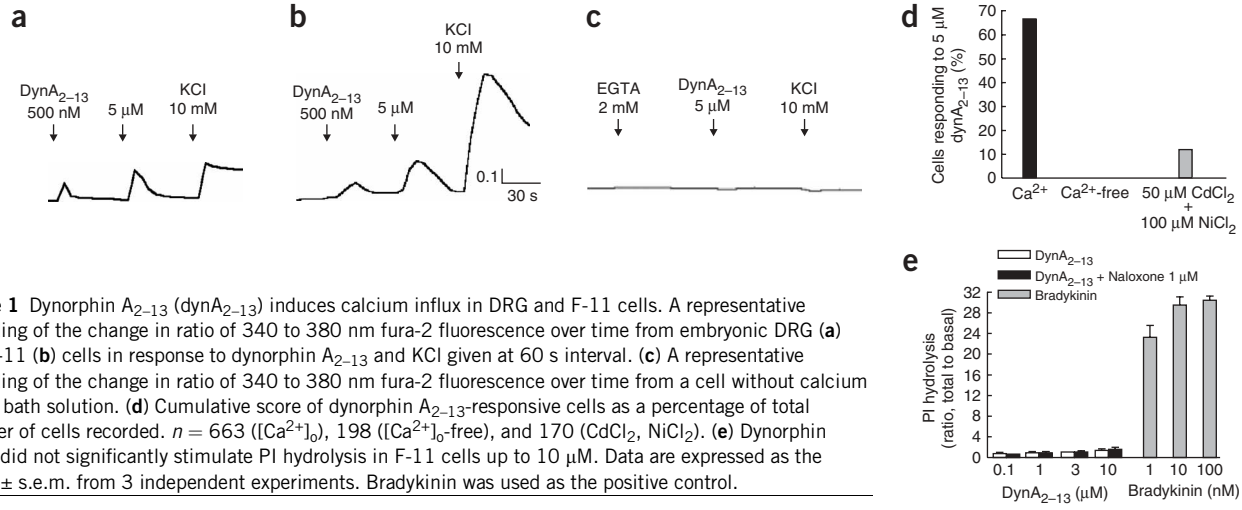

Figure 1 Dynorphin $A_{2–13}$ ($dynA_{2–13}$) induces calcium influx in DRG and F-11 cells. A representative recording of the change in ratio of 340 to 380 nm fura-2 fluorescence over time from embryonic DRG (**a**) and F-11 (**b**) cells in response to dynorphin $A_{2–13}$ and KCl given at 60 s interval. (**c**) A representative recording of the change in ratio of 340 to 380 nm fura-2 fluorescence over time from a cell without calcium in the bath solution. (**d**) Cumulative score of dynorphin $A_{2–13}$-responsive cells as a percentage of total number of cells recorded. $n = 663$ ($[Ca^{2+}]_o$), 198 ($[Ca^{2+}]_o$-free), and 170 ($CdCl_2$, $NiCl_2$). (**e**) Dynorphin $A_{2–13}$ did not significantly stimulate PI hydrolysis in F-11 cells up to 10 μM. Data are expressed as the mean ± s.e.m. from 3 independent experiments. Bradykinin was used as the positive control.

$A_{1–17}$ (500 nM and 5 μM) had a small effect on $[Ca^{2+}]_i$ in F-11 cells (8.3% responsive cells at 5 μM, $n = 36$). In the presence of 1 μM naloxone, 9.4% cells responded to dynorphin $A_{1–17}$ ($n = 149$), which was not significantly different from responses in the absence of naloxone.

The effect of dynorphin $A_{2–13}$ was abolished by eliminating extracellular Ca^{2+} (**Fig. 1c**). Of 198 recorded cells, none responded to 5 μM dynorphin $A_{2–13}$. Blockade of calcium influx by 50 μM $CdCl_2$ and 100 μM $NiCl_2$ had a similar effect; only 21 of 170 (12%) recorded cells responded to 5 μM dynorphin $A_{2–13}$ compared with 67% cells in normal medium (**Fig. 1d**). The increase in $[Ca^{2+}]_i$ observed in the 21 cells was also significantly smaller than that in normal medium (ratio of 340 to 380 nm, 0.09 ± 0.04 and 0.30 ± 0.09, respectively, $P = 0.0001$). The increase in $[Ca^{2+}]_i$ was not due to the activation of the phospholipase C (PLC_β) pathway to promote calcium release from intracellular stores because unlike bradykinin, dynorphin $A_{2–13}$ did not stimulate the production of inositol phosphates in F-11 cells (**Fig. 1e**). Thus dynorphin A induced a transient increase in $[Ca^{2+}]_i$ by calcium influx that was independent of opioid receptors. These effects of dynorphin A occurred at doses (500 nM to 5 μM) that are more than 100 times lower than the excitotoxic doses of dynorphin A on cultured neurons[13].

The dynorphin-induced calcium influx was sensitive to VSCC inhibitors. The L-type channel blocker, nimodipine, and the P/Q-type channel blocker, ω-agatoxin TK, significantly reduced the percent of F-11 cells that responded to dynorphin $A_{2–13}$ (**Fig. 2**). The concentration ranges of nimodipine[24] and ω-agatoxin TK[25] used are selective for the respective calcium channel subtypes. The N-type channel blocker, ω-conotoxin GVIA (300 nM to 3 μM), the T-type channel blocker ethosuximide (300 nM to 3 μM), the non-selective calcium channel blocker flunarizine (300 nM to 3 μM) and the NMDA receptor antagonist MK-801 (30 μM) had no effect on dynorphin A-induced increase in $[Ca^{2+}]_i$.

A series of agonists and antagonists for receptors that are found in the DRG were tested for possible inhibition of dynorphin $A_{2–13}$-induced calcium influx. Of these, only the bradykinin B2 receptor selective antagonist D-Arg-[Hyp3, Thi5, D-Tic7, Oic8]-bradykinin (HOE 140) completely abolished the dynorphin-induced $[Ca^{2+}]_i$ with an IC_{50} of 2.8 nM (log IC_{50} ± s.e.m. = –8.56 ± 0.52; **Fig. 3a**), which is consistent with the affinity of HOE 140 for the B2 receptor[26],

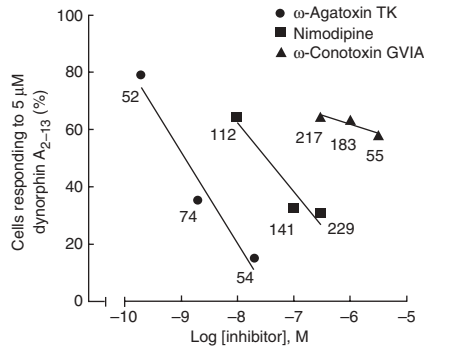

Figure 2 Inhibitory effect of VSCC blockers on dynorphin $A_{2–13}$-induced $[Ca^{2+}]_i$ in F-11 cells. Data are expressed as the percent of F-11 cells that responded to 5 μM dynorphin $A_{2–13}$ alone. The total number of cells recorded per data point is indicated. The IC_{50} of ω-agatoxin TK and nimodipine are 2.9 nM ($r^2 = 0.96$) and 107 nM ($r^2 = 0.93$) based on linear regression analysis.

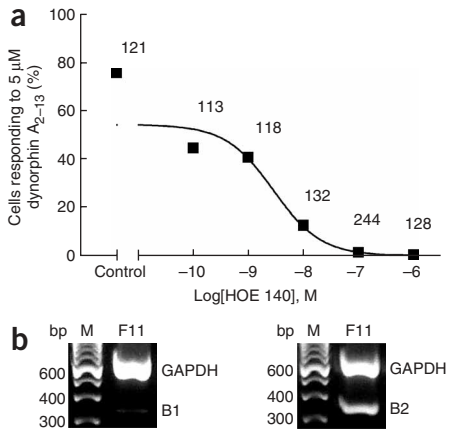

Figure 3 Inhibitory effect of B2 receptor–selective antagonist HOE 140 on dynorphin $A_{2–13}$-induced $[Ca^{2+}]_i$ in F-11 cells that express predominantly B2 receptors. (**a**) Dose-effect of HOE 140 on dynorphin $A_{2–13}$-induced $[Ca^{2+}]_i$. The total number of cells recorded per data point is indicated. (**b**) Multiplex RT-PCR of F-11 cells confirming expression of endogenous B2 receptors. GAPDH was co-amplified as an internal loading control. Left, *Bdkrb1* product (B1), 334 bp; right, *Bdkrb2* product (B2), 346 bp. GAPDH, 638 bp. M, 100-bp DNA ladder marker (Invitrogen).

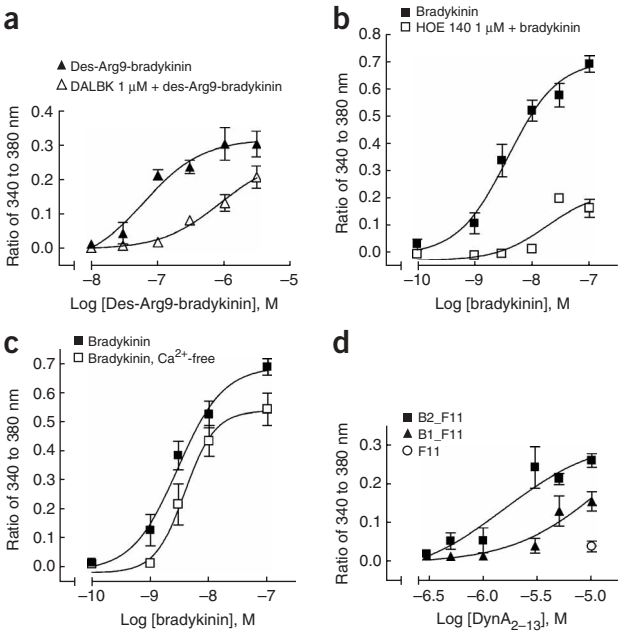

Figure 4 Heterologous expression of human B1 or human B2 receptors in F-11 cells that have spontaneously lost responsiveness to dynorphin A. (**a**) B1 receptor agonist des-Arg9-BK induced an increase in $[Ca^{2+}]_i$ in *BDKRB1*-transfected cells. The effect was blocked by the B1 selective antagonist DALBK (1 μM). (**b**) Bradykinin induced an increase in $[Ca^{2+}]_i$ in *BDKRB2*-transfected cells. The effect was blocked by the B2 selective antagonist HOE 140 (1 μM). (**c**) Bradykinin induced $[Ca^{2+}]_i$ in the *BDKRB2* transfected cells was reduced in the absence of extracellular calcium. (**d**) Transfection of either *BDKRB1* (closed triangles) or *BDKRB2* (closed squares) was sufficient to restore the responsiveness to dynorphin $A_{2–13}$ in F-11 cells (open circles) that had spontaneously lost responsiveness to dynorphin A. Data are plotted as mean ± s.e.m. of change in ratio of 340 to 380 nm; total number of cells recorded per data point ranged from 55 to 150 from multiple wells.

suggesting that dynorphin A activates calcium influx in F-11 cells through an agonist action at the B2 receptor. We confirmed the expression of B2 receptors[22] by RT-PCR and found very little B1 receptor transcript (**Fig. 3b**). In addition, H89, an inhibitor of protein kinase A (PKA, 1 μM) completely blocked the effect of dynorphin $A_{2–13}$ ($n = 71$). Hence, dynorphin $A_{2–13}$ activated the B2 receptor to activate the L-type and P/Q-type VSCC by a PKA-dependent pathway. Modulation of VSCC by G-proteins and protein kinases is well documented[27–30]. The G_s-cAMP-PKA pathway augments both L-type and N-type current in neuronal tissues[27]. Whether dynorphin A activates B2 receptor coupling to the G_s-cAMP-PKA pathway to activate calcium influx remains to be determined; B2 receptor coupling to the cAMP pathway occurs under some conditions[31].

We further examined the potential agonist actions of dynorphin A at the B1 and B2 receptors by transfecting cultures of F-11 cells that had spontaneously lost the ability to respond to dynorphin $A_{2–13}$ (up to 10 μM) with the cDNA for the human bradykinin B1 (*BDKRB1*) or B2 (*BDKRB2*) receptor. Transfected cells constitutively expressed either *BDKRB1* or *BDKRB2* mRNA (**Supplementary Fig. 4** online). The functional expression of the human B1 or the human B2 receptor was confirmed, respectively, by the dose-dependent effect of the B1 selective agonist, des-Arg9-bradykinin (EC_{50} = 62 nM; log EC_{50} ± s.e.m. = –7.2 ± 0.28) or bradykinin (EC_{50} = 3.8 nM; log EC_{50} ± s.e.m. = –8.4 ± 0.12) on $[Ca^{2+}]_i$ and by respective inhibition by the B1 antagonist, [Des-Arg9, Leu8]bradykinin (DALBK)[32] or the B2 antagonist HOE 140 (**Fig. 4a**,**b**)[32]. Increase in $[Ca^{2+}]_i$ by bradykinin receptors is thought to be primarily due to mobilization of intracellular stores[26,33] and partly due to calcium influx[34–36]. Consistent with these earlier observations, depletion of extracellular calcium slightly attenuated (~20%) the effect of bradykinin at the transfected human B2 receptor (**Fig. 4c**). The EC_{50} values of bradykinin in control versus calcium-free medium were 2.9 nM (log EC_{50} ± s.e.m. = –8.5 ± 0.13) and 3.9 nM (log EC_{50} ± s.e.m. = –8.4 ± 0.12), respectively, and the E_{max} values were 0.69 ± 0.06 and 0.54 ± 0.05, respectively. Expression of either the human B1 or human B2 receptor fully restored the cells' response to dynorphin $A_{2–13}$ (**Fig. 4d**). The larger response observed in cells expressing the human B2 receptor correlated with its higher expression (see below). The estimated EC_{50} value for dynorphin $A_{2–13}$ was 1.5 μM (log EC_{50} ± s.e.m. = –5.81 ± 0.34) for the human B2 receptor, and this dose effect was completely blocked by 1 μM HOE 140 (**Supplementary Fig. 5** online). The dose-response curve for dynorphin $A_{2–13}$ in the *BDKRB1* transfected cells (**Fig. 4d**) did not reach saturation statistically, possibly due to lower expression of the human B1 receptor (see below), a lower potency of dynorphin $A_{2–13}$ at the human B1 receptor, or both. These data demonstrate that the B1 or the B2 receptor is sufficient to mediate the dynorphin A-induced calcium influx, which is distinct from the mainly intracellular calcium mobilizing effect of bradykinin.

Dynorphin A directly interacts with B1 and B2 receptors

Saturation binding using [^{3}H]bradykinin showed a K_D of 2.0 ± 0.35 nM ($n = 3$) and a B_{max} of 1,030 ± 260 fmol mg^{-1} in human B2 receptor-expressing cells. As bradykinin has a significantly lower affinity for the B1 receptor[37], [^{3}H]kallidin was used to characterize the human B1 receptor. The K_D of [^{3}H]kallidin at the human B1 receptor was 2.2 ± 1.27 nM ($n = 3$), and the B_{max} was 385 ± 14.4 fmol mg^{-1}. Dynorphin $A_{2–13}$ competed for [^{3}H]bradykinin binding with apparent affinity ranging from 1.4 μM to 2.0 μM at the

Table 1 Competitive radioligand binding analysis of dynorphin $A_{2–13}$ and dynorphin $A_{1–17}$ against [^{3}H]bradykinin or [^{3}H]kallidin in various cell lines and mouse brain tissues

		Dynorphin $A_{2–13}$			Dynorphin $A_{1–17}$		
Radioligand	Tissue	Log IC_{50} ± s.e.m.[g]	K_i (nM)[h]	*n*	Log IC_{50} ± s.e.m.[g]	K_i (nM)[h]	*n*
[^{3}H]bradykinin[a]	F-11[c]	–5.58 ± 0.08	2,000	4	–5.75 ± 0.17	1,400	3
	B2_F11[d]	–5.58 ± 0.08	2,000	2			
	COS-7[c]	–5.63 ± 0.18	1,800	8			
	Mouse brain (WT)[e]	–5.56 ± 0.14	2,100	3			
	Mouse brain (*Bdkrb1*$^{-/-}$)[f]	–5.73 ± 0.16	1,400	2			
[^{3}H]kallidin[b]	B1_F11[d]	–5.56 ± 0.07	2,100	3			

[a]The K_D value of [^{3}H]bradykinin based on saturation analysis using membranes from transfected F-11 cells expressing the human B2 receptor is 2.0 ± 0.35 nM ($n = 3$). [b]The K_D value of [^{3}H]kallidin based on saturation analysis using membranes from transfected F-11 cells expressing the human B1 receptor is 2.2 ± 1.27 nM ($n = 3$). [c]The rodent F-11 cells and the simian COS-7 cells express endogenous B2 receptors. [d]F-11 cells were stably transfected with cDNA for either the human B1 receptor (B1_F11) or the human B2 receptor (B2_F11). [e]Mouse whole-brain membranes were prepared from wild-type littermates of mice that carried a null mutation of the B1 receptor (*Bdkrb1*$^{-/-}$). [f]Mouse whole-brain membranes were prepared from *Bdkrb1*$^{-/-}$ mice. [g]The log IC_{50} ± standard error of the mean (s.e.m.) of dynorphin $A_{2–13}$ and dynorphin $A_{1–17}$ was determined by non-linear regression analysis of data collected from multiple independent experiments (*n*). [h]The K_i value was calculated from the anti-logarithmic value of the IC_{50} by the Cheng and Prusoff equation based on the K_D value of the respective radioligand and concentration range of 600–650 pM.

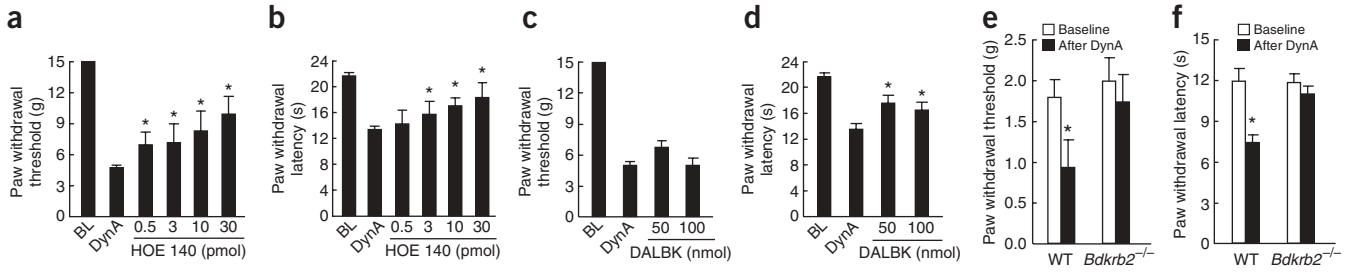

Figure 5 Effects of HOE 140 and DALBK on tactile hypersensitivity and thermal hyperalgesia induced by dynorphin $A_{2–13}$. Decreased tactile (**a**) and thermal (**b**) thresholds in rats 60 min after treatment with intrathecal dynorphin $A_{2–13}$ (3 nmol; $n = 5$-8). (**c**,**d**) Effect of DALBK on tactile (**c**) and thermal (**d**) hypersensitivities produced by dynorphin $A_{2–13}$ ($n = 5$-8). (**e**,**f**) Effect of dynorphin $A_{2–13}$ (intrathecal, 3 nmol) on tactile (**e**) and thermal (**f**) hypersensitivities in wild-type (WT) and *Bdkrb2*$^{-/-}$ mice at 60 min after administration of dynorphin $A_{2–13}$ (intrathecal, 3 nmol; $n = 7$). *$P < 0.05$.

rodent B2 (in F-11 and brain membranes from both wild-type and *Bdkrb1*$^{-/-}$ mice[38]) and primate B2 (in COS-7 and *BDKRB2* transfected cells; **Table 1**). For the human B1 receptor, dynorphin $A_{2–13}$ had an apparent affinity of 1.5 μM based on competition with [^{3}H]kallidin. Thus, dynorphin $A_{2–13}$ showed similar affinity for both bradykinin receptor types. The opioid dynorphin $A_{1–17}$ had similar affinity for the [^{3}H]bradykinin binding site as dynorphin $A_{2–13}$. Competitive binding analysis against [^{3}H]bradykinin or [^{3}H]kallidin provides an estimation of dynorphin's affinity for the bradykinin receptors. The different functional coupling of the bradykinin receptor activated by bradykinin versus by dynorphin *in vitro* suggests that dynorphin and bradykinin may interact differently with these receptors; if so, the indirect binding analysis may underestimate the affinity of dynorphin for bradykinin receptors.

Bradykinin antagonists block dynorphin A-induced pain

We then examined whether agonist actions at the bradykinin receptors underlies the pronociceptive effect of dynorphin A. Intrathecal administration of dynorphin $A_{2–13}$ (3 nmol) into the lumbar region of rats induced significant reversible hypersensitivity to innocuous touch (tactile hypersensitivity) and noxious heat (thermal hyperalgesia) in the hind paw within 30 min after the injection (**Fig. 5a–d**). The baseline paw-withdrawal thresholds diminished from 15.00 ± 0.0 g to 4.8 ± 0.3 g ($P = 6.75 \times 10^{-22}$) (**Fig. 5a**,**c**), whereas the paw withdrawal latency to noxious radiant heat decreased from 22 ± 0.5 s to 13 ± 0.6 s ($P = 5.08 \times 10^{-11}$) (**Fig. 5b**,**d**). Intrathecal HOE 140 produced a significant dose-dependent reversal of tactile hypersensitivity ($P = 0.003$) (**Fig. 5a**) and of thermal hyperalgesia ($P = 0.03$; **Fig. 5b**) induced by dynorphin $A_{2–13}$. At the highest dose tested (30 pmol), paw withdrawal thresholds increased to 9.9 ± 1.7 g (**Fig. 5a**) and paw withdrawal latencies to radiant heat increased to 18.4 ± 2.3 s (**Fig. 5b**). In contrast, DALBK had no effect on tactile hypersensitivity over the dose range tested ($P = 0.09$) (**Fig. 5c**) and partially reversed thermal hyperalgesia ($P = 0.02$; **Fig. 5d**). B2 receptors are the predominant bradykinin receptor type in DRG neurons and spinal cord in adult rats[39], though functional B1 receptors exist in the DRG and spinal cord of normal adult rat[40,41]. However, we found no evidence for kininogen transcripts in the spinal cord (see below), and there is no published evidence supporting a role of bradykinin as a neurotransmitter. Hence, indirect mediation of pronociceptive effects of exogenous dynorphin A through bradykinin receptors subsequent to local release of bradykinin is unlikely. These data suggest that intrathecal dynorphin $A_{2–13}$ is pronociceptive, and that this effect is mediated directly by the B2 receptor.

This conclusion was further substantiated by comparing the effect of intrathecal dynorphin $A_{2–13}$ in transgenic mice that lack the B2 receptor (*Bdkrb2*$^{-/-}$) and their wild-type littermates (**Fig. 5e,f**). Intrathecal injection of 3 nmol of dynorphin $A_{2–13}$ in the spinal cord similarly induced significant tactile hypersensitivity (baseline value reduced from 1.8 ± 0.2 g to 0.9 ± 0.3 g; $P = 0.02$)(**Fig. 5e**) and thermal hyperalgesia (baseline value reduced from 12.0 ± 0.8 s to 7.4 ± 0.6 s; $P = 0.028$) (**Fig. 5f**) in the wild-type mice within 1 h after dynorphin injection. These effects of dynorphin $A_{2–13}$ were not observed in the *Bdkrb2*$^{-/-}$ mice, suggesting that the presence of B2 receptor in the spinal cord is necessary for the pronociceptive action of pharmacological dynorphin A.

Upregulation of spinal dynorphin may be critical in maintaining neuropathic pain states[17,20,42]. This led us to examine whether the action of endogenous dynorphin A at bradykinin receptors may underlie pain induced by nerve injury. Behavioral signs of neuropathic pain were well established within two days after unilateral lumbar L5 and L6 spinal nerve ligation (SNL) and persisted for many weeks[43]. The mean paw withdrawal threshold to probing with von Frey filaments in rats with SNL significantly ($P = 5.9 \times 10^{-35}$) decreased from a pre-SNL baseline of 15 ± 0 g to 3.6 ± 0.4 g, and the mean paw withdrawal latency to noxious radiant heat was significantly ($P = 3.5 \times 10^{-15}$) decreased from a pre-SNL baseline of 20 ± 0.5 s to 13 ± 0.4 s (**Fig. 6**). The spinal administration of 0.5 pmol of HOE 140 on day 2, 4, 7, 10 or 14 after

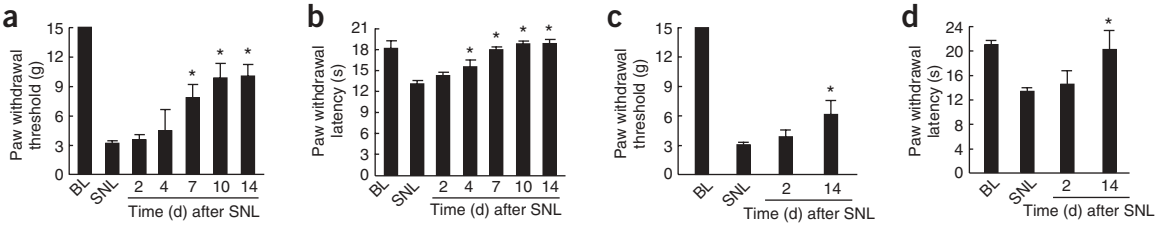

Figure 6 Effects of intrathecal bradykinin receptor antagonists on the tactile and thermal hypersensitivities induced by L5–L6 SNL ($n = 6$–7). (**a**,**b**) Effect of intrathecal administration of HOE 140 (0.5 pmol) on tactile (**a**) and thermal (**b**) hypersensitivities at day 2, 4, 7, 10, 14 after L5–L6 SNL. (**c**,**d**) Effect of intrathecal administration of 50 nmol of DALBK on tactile (**c**) and thermal hypersensitivities (**d**) at day 2 and day 14 after L5–L6 SNL. *$P < 0.05$.

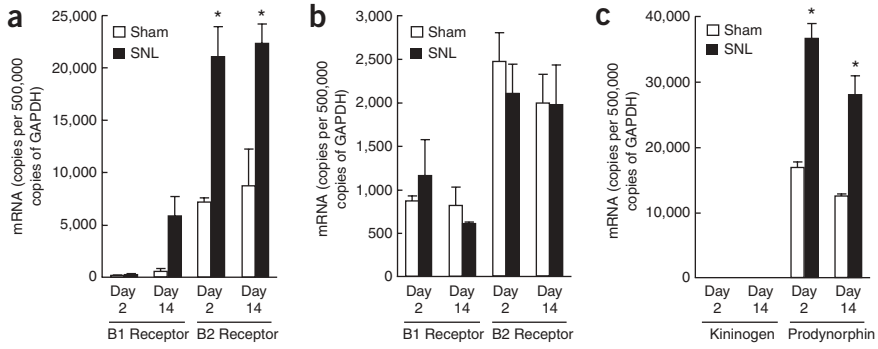

Figure 7 Quantitative PCR analysis of bradykinin receptor, kininogen and prodynorphin transcripts in the DRG and spinal cord of sham control and L5–L6 SNL rats ($n = 6$). (**a**) B1 and B2 receptor mRNA in the ipsilateral L5 DRG at day 2 and day 14 after sham surgery or L5–L6 SNL. (**b**) B1 and B2 receptor mRNA in the ipsilateral dorsal horn of the lumbar spinal cord from rats at day 2 and day 14 after sham-surgery or L5–L6 SNL. (**c**) Spinal kininogen and prodynorphin mRNA at day 2 and day 14 after sham-surgery or L5–L6 SNL. $^*P < 0.05$.

SNL produced a significant time-dependent reversal of tactile hypersensitivity ($P = 2.23 \times 10^{-8}$) and of thermal hyperalgesia ($P = 5.5 \times 10^{-8}$) over 14 days (**Fig. 6a**,**b**). Although no reversal occurred 2 days after SNL, a maximal reversal of tactile hypersensitivity by HOE 140 occurred on day 14 (10 ± 1.3 g) after SNL (**Fig. 6a**). Similarly, a complete reversal of thermal hyperalgesia by intrathecal HOE 140 (to 18 ± 0.37 s) occurred by day 7 after SNL but not earlier (**Fig. 6b**). Administration of HOE 140 did not alter behavioral responses of sham-operated rats (data not shown).

The time dependence of the B2 antagonist effect is consistent with our previous work showing that SNL injury results in a time-dependent upregulation of spinal dynorphin, which has a delayed onset and does not reach significance until day 4 after SNL, peaking at approximately 7 to 10 days after injury[17]. The reversal of neuropathic pain by HOE 140 suggests that spinal B2 receptor activation is critical for maintaining, but not initiating, SNL-induced pain states. Studies using knockout mice that lack prodynorphin[20] also show that dynorphin is necessary for the maintenance but not the onset of neuropathic pain. Thus, the reversal of neuropathic pain by intrathecal B2 receptor antagonist occurs only when spinal dynorphin is elevated and at a time when the hyperalgesia can be blocked by the intrathecal injection of an antiserum to dynorphin[17,20]. Together with the *in vitro* data demonstrating that dynorphin A directly activates bradykinin receptors, and the lack of pronociceptive activity of dynorphin in *Bdkrb2*$^{-/-}$ mice, these studies demonstrate physiological relevance of the action of dynorphin A at the B2 receptor in neuropathic pain states.

Similar studies were done with intrathecal injection of DALBK (50 nmol) 2 and 14 days after SNL (**Fig. 6c**,**d**). A moderate but significant ($P = 0.046$) reversal of tactile hypersensitivity was seen 14 days after SNL (6.2 ± 1.5 g, **Fig. 6c**). Thermal hyperalgesia was fully reversed ($P = 0.03$) by DALBK 14 days after SNL (20 ± 3.2 s, **Fig. 6d**). Neither tactile nor thermal hypersensitivity was altered by DALBK given 2 days after SNL. The weak effect of DALBK (**Fig. 6c**) is likely to be due to the lower level of expression of the B1 receptor (**Fig. 7a**,**b**) in both sham and SNL-injured rats.

Upregulation of B1 and B2 receptor expression was observed only in the injured L5 DRG (**Fig. 7a**) but not in the lumbar spinal cord (**Fig. 7b**) after SNL. Moreover, upregulation of the expression of the B1 receptor occurred only on day 14, but not on day 2, whereas upregulation of expression of the B2 receptor was evident by day 2 (**Fig. 7a**). Despite this predominant expression of the B2 receptor in the spinal cord and DRG on day 2 after SNL, when both tactile and thermal hypersensitivity were evident, spinal HOE 140 did not reverse the abnormal pain state, suggesting that upregulation of the B2 receptor alone is not sufficient to contribute to the onset of neuropathic pain. This observation suggests that the role of the spinal B2 receptor in the maintenance but not the initiation of neuropathic pain states requires alterations in transmitter activity, that is, spinal dynorphin, acting at the B2 receptor.

Quantitative RT-PCR of spinal cord tissues from these experimental animals showed very low levels of kininogen mRNA, the precursor for bradykinin, in both sham control and nerve injured rats, suggesting that there is little *de novo* bradykinin in the spinal cord (**Fig. 7c**). In contrast, prodynorphin transcripts were readily measured. Prodynorphin was upregulated by day 2 (**Fig. 7c**) preceding an upregulation of spinal dynorphin (> day 4)[17] as is expected of the precursor for dynorphin. The failure of the bradykinin receptor antagonists to reverse SNL-induced pain at early time points after injury greatly diminishes the possibility that bradykinin in the spinal cord from the circulation mediates the hypersensitivity to evoked pain as tested here.

DISCUSSION

Dynorphin A's dual actions as an endogenous opioid and bradykinin receptor agonist represent the identification of a neuropeptide that can activate two classes of G protein-coupled receptors with diverse structure and function. The different structure-activity relationship of dynorphin A at opioid receptors (N-terminal tyrosine is essential) and bradykinin receptors (N-terminal tyrosine is unnecessary) is consistent with the peptide's interaction with two structurally and pharmacologically distinct receptors. We have shown that dynorphin $A_{2–13}$ enhances capsaicin-evoked CGRP release from the central terminals of the primary afferent in the dorsal horn of the spinal cord[44]. The activation of VSCC by dynorphin A via the B2 receptor is consistent with the potentiating effect of dynorphin A on CGRP release from the central terminals of the primary afferent and represents a possible mechanism of hyperalgesia induced by spinal dynorphin. The apparent affinity and potency of dynorphin A for the bradykinin receptors are moderate, suggesting that activation of the bradykinin receptors by endogenous dynorphin A may require close apposition of dynorphin A-containing terminals with dendritic or cell surface bradykinin receptors and sufficient levels of dynorphin A. In the dorsal horn of the spinal cord, bradykinin receptors are largely associated with the central terminals of the primary afferents in the superficial laminae[40,45], where prodynorphin interneurons are also located[20,46]. Intrathecal administration of dynorphin A mimicked the release of dynorphin in the spinal cord and was pronociceptive; this effect was blocked by antagonists for the bradykinin receptors administered locally in the spinal cord. The antihyperalgesic effect of intrathecal B1 and B2 receptor antagonists in a model of peripheral neuropathy may be due to activation of these receptors by the enhanced level of spinal dynorphin induced by the injury. These findings implicate that selective antagonism against dynorphin A at bradykinin receptors blocks the pronociceptive actions of spinal dynorphin without interfering with essential peripheral function of bradykinin or of dynorphin A at the opioid receptors. These findings represent a new mechanism for the

excitatory actions of dynorphin and offer possibilities for the development of therapeutic strategies for the treatment of pain.

METHODS

Cell culture. F-11 cells (gift from M. Fishman) were maintained as described[21]. Cell differentiation was initiated 72 h before assay. Embryonic DRG neurons were isolated from E15–17 rats, plated at 150,000 cells per Delta-T dish (Bioptechs) as described[34] and assayed between day 9 and 12 after plating. F-11 cells were transfected with the *BDKRB1*or *BDKRB2* cDNA (UMR cDNA Resource Center) using PolyFect (Qiagen) and selected with 1 mg ml^{-1} G418 (Invitrogen).

$[Ca^{2+}]_i$ measurement. F-11 cells were plated at 50,000 cells per 8 mm cloning ring sealed onto a Delta-T dish (Bioptechs) and differentiated 24 h after plating. For each experiment, cells were loaded with 5 μM fura-2/AM (Molecular Probes) at 37 °C for 40 min in bathing solution: 136 mM NaCl, 5.4 mM KCl, 2 mM $CaCl_2$, 1 mM $MgSO_4$, 5.5 mM glucose, 10 mM HEPES, pH 7.4. Image acquisition was done at 37 °C using a Nikon TE200 outfitted with a plan fluor ×40 oil N.A. 1.3 objective lens, Xenon burner, an ORCA Hi binning 12 bit digital camera, filter wheel with fura-2 filter set controlled by Mutech image master digital workstation and Metafluor imaging software (Universal Imaging). Ratiometric fluorescence images were captured at 6 s intervals by alternate excitation at 340 nm and 380 nm, with emission at 510 nm. The fluorescence of Fura-2 associated with individual cells was determined by computer-assisted analysis using Metafluor imaging software. A cell area within a digital image was delineated, and the optical density associated with the cell area was expressed as a ratio of integrated optical density emitted at 510 nm after excitation at 340 nm versus 380 nm. The calculated ratios associated with the same cell area derived from the serial images were plotted over time (s). Increases over the basal ratio over time produced an area under the curve representing total enhanced fluorescence within that cell, whereas the peak ratio represented the maximal amplitude of the response. For non-transfected F-11 cells and primary DRG neurons, a cell was defined as responsive if an area under the curve was detected; the effect of a drug was expressed as an overall response of a population of cells (percent of cells responding to dynorphin $A_{2–13}$) and not by the mean peak amplitude of the response. This is because F-11 cells are heterogeneous, resulting in a large variance in the peak amplitude among responding cells within a population. For transfected cells, because the receptor expression is higher and more consistent, the variance of the peak amplitude of a cell within a population is smaller, enabling the effect of a drug to be expressed as mean peak amplitude of the response, that is, peak change in ratio of 340 to 380 nm. Dose-response curves were fitted by nonlinear least-squares analysis (GraphPad Prism).

[^{3}H]phosphatidylinositol hydrolysis assay. F11 cells were plated at 200,000 cells per well in 24-well titer plates and analyzed as described[47]. Data are mean ± s.e.m. of three independent experiments. Statistical difference (95% C.L.) was determined by student *t*-test.

Animals. Male Sprague-Dawley rats (Harlan) weighing 225–300 g, and male bradykinin B2 receptor knockout (*Bdkrb2*$^{-/-}$) mice (B6; 129S7-Bdkrb2^{tm1jfh}/J) and the corresponding wild-type control mice (B6; 129SF2/J; Jackson Laboratory) were used. Animals were maintained in cages in a climate-controlled room on a 12-h light-dark cycle with free access to food and water. All testing procedures were done in accordance with the policies and recommendations of the International Association for the Study of Pain and the National Institutes of Health guidelines for the handling and use of laboratory animals and were approved by the Institutional Animal Care and Use Committee of the University of Arizona.

Cannulation and drug administration. Rats were anesthetized with ketamine (80 mg per kg body weight) and xylazine (12 mg kg^{-1}) and implanted with intrathecal catheters directed to the lumbar spinal cord[48]. Drug or vehicle injections (5 μl) were followed by a 9 μl saline flush. Drugs used were DALBK (Bachem Inc.), HOE 140 (American Peptide Company) and dynorphin $A_{2–13}$ (AnaSpec Inc.). Intrathecal injections to conscious mice were made by direct lumbar (L5–L6) puncture into the subarachnoid space.

Spinal nerve ligation. Spinal nerve ligation was done as described[43] in rats anesthetized with 0.5% halothane in 95%O_2, 5% CO_2. Sham-operated control rats were prepared in an identical manner but without nerve ligation.

Behavioral testing. All behavioral testing was done by observers blinded to the experimental conditions. Tactile hypersensitivity was determined by probing the plantar surface of the ligated hind paw with a series of eight calibrated von Frey filaments (0.40, 0.70, 1.2, 2.0, 3.63, 5.5, 8.5, and 15 g)[49]. The paw withdrawal thresholds of mice were determined in the same manner but using von Frey filaments over a range of 0.02 to 2.34 g. Thermal sensitivity of animals was determined by the withdrawal latency to an infrared heat source directed onto the plantar surface of the left hind paw and was indicated by a motion detector that halted the source and a timer[50]. A maximum cut-off of 33 s was used. The latencies were measured before surgery, before and after drug or vehicle administration. The results are presented as the mean ± s.e.m. Student's *t*-test, one-way ANOVA, two-factor ANOVA for independent variables followed by Fisher's least significant difference post-hoc test were used where appropriate. In all statistical comparisons, $P < 0.05$ was used as the criterion for statistical significance.

Quantitative RT-PCR was performed using the iCycler iQ Multicolor Real-Time PCR Detection System with iScript cDNA Synthesis Kit and iQ SYBR Green Supermix (Bio-Rad). Samples were run in triplicate using an annealing temperature of 60°C. See **Supplementary Methods** online for primer sequences. Data are mean ± s.e.m. of 3 independent tissue samples.

Note: Supplementary information is available on the Nature Neuroscience website.

ACKNOWLEDGMENTS

This work was supported by a grant from the National Institute on Drug Abuse. The authors appreciate the technical assistance of Y. Kawamoto on DRG cultures and H. Badghisi on the PI hydrolysis assay.

AUTHOR CONTRIBUTIONS

M.-C.L. conducted the ratiometric imaging, designed and executed the PCR analyses, performed the data analysis and prepared the figures. Q.C. conducted the surgeries and behavioral experiments and data analysis.

COMPETING INTERESTS STATEMENT

The authors declare that they have no competing financial interests.

Published online at http://www.nature.com/natureneuroscience
Reprints and permissions information is available online at http://npg.nature.com/reprintsandpermissions/

1. Beaumont, A. & Hughes, J. Biology of opioid peptides. *Annu. Rev. Pharmacol. Toxicol.* **19**, 245–267 (1979).
2. Goldstein, A., Tachibana, S., Lowney, L.I., Hunkapiller, M. & Hood, L. Dynorphin-(1–13), an extraordinarily potent opioid peptide. *Proc. Natl. Acad. Sci. USA* **76**, 6666–6670 (1979).
3. Quirion, R. & Pilapil, C. Opioid receptor binding profile of [3H]dynorphin A-(1–8) in rat and guinea pig brain. *Eur. J. Pharmacol.* **99**, 361–363 (1984).
4. Chavkin, C., James, I.F. & Goldstein, A. Dynorphin is a specific endogenous ligand of the kappa opioid receptor. *Science* **215**, 413–415 (1982).
5. Corbett, A.D., Paterson, S.J., McKnight, A.T., Magnan, J. & Kosterlitz, H.W. Dynorphin and dynorphin are ligands for the kappa-subtype of opiate receptor. *Nature* **299**, 79–81 (1982).
6. Zhang, S. *et al.* Dynorphin A as a potential endogenous ligand for four members of the opioid receptor gene family. *J. Pharmacol. Exp. Ther.* **286**, 136–141 (1998).
7. Herman, B.H. & Goldstein, A. Antinociception and paralysis induced by intrathecal dynorphin A. *J. Pharmacol. Exp. Ther.* **232**, 27–32 (1985).
8. Walker, J.M., Moises, H.C., Coy, D.H., Baldrighi, G. & Akil, H. Nonopiate effects of dynorphin and des-Tyr-dynorphin. *Science* **218**, 1136–1138 (1982).
9. Faden, A.I. & Jacobs, T.P. Dynorphin-related peptides cause motor dysfunction in the rat through a non-opiate action. *Br. J. Pharmacol.* **81**, 271–276 (1984).
10. Stevens, C.W., Weinger, M.B. & Yaksh, T.L. Intrathecal dynorphins suppress hindlimb electromyographic activity in rats. *Eur. J. Pharmacol.* **138**, 299–302 (1987).
11. Vanderah, T.W. *et al.* Single intrathecal injections of dynorphin A or des-Tyr-dynorphins produce long-lasting allodynia in rats: blockade by MK-801 but not naloxone. *Pain* **68**, 275–281 (1996).
12. Koetzner, L., Hua, X.Y., Lai, J., Porreca, F. & Yaksh, T. Nonopioid actions of intrathecal dynorphin evoke spinal excitatory amino acid and prostaglandin E2 release mediated by cyclooxygenase-1 and -2. *J. Neurosci.* **24**, 1451–1458 (2004).

13. Skilling, S.R., Sun, X., Kurtz, H.J. & Larson, A.A. Selective potentiation of NMDA-induced activity and release of excitatory amino acids by dynorphin: possible roles in paralysis and neurotoxicity. *Brain Res.* **575**, 272–278 (1992).
14. Tang, Q., Lynch, R.M., Porreca, F. & Lai, J. Dynorphin A elicits an increase in intracellular calcium in cultured neurons via a non-opioid, non-NMDA mechanism. *J. Neurophysiol.* **83**, 2610–2615 (2000).
15. Hauser, K.F., Foldes, J.K. & Turbek, C.S. Dynorphin A (1–13) neurotoxicity in vitro: opioid and non-opioid mechanisms in mouse spinal cord neurons. *Exp. Neurol.* **160**, 361–375 (1999).
16. Ruda, M.A., Iadarola, M.J., Cohen, L.V. & Young, W.S., III. In situ hybridization histochemistry and immunocytochemistry reveal an increase in spinal dynorphin biosynthesis in a rat model of peripheral inflammation and hyperalgesia. *Proc. Natl. Acad. Sci. USA* **85**, 622–626 (1988).
17. Malan, T.P. *et al.* Extraterritorial neuropathic pain correlates with multisegmental elevation of spinal dynorphin in nerve-injured rats. *Pain* **86**, 185–194 (2000).
18. Schwei, M.J. *et al.* Neurochemical and cellular reorganization of the spinal cord in a murine model of bone cancer pain. *J. Neurosci.* **19**, 10886–10897 (1999).
19. Vanderah, T.W. *et al.* Dynorphin promotes abnormal pain and spinal opioid antinociceptive tolerance. *J. Neurosci.* **20**, 7074–7079 (2000).
20. Wang, Z. *et al.* Pronociceptive actions of dynorphin maintain chronic neuropathic pain. *J. Neurosci.* **21**, 1779–1786 (2001).
21. Platika, D., Boulos, M.H., Baizer, L. & Fishman, M.C. Neuronal traits of clonal cell lines derived by fusion of dorsal root ganglia neurons with neuroblastoma cells. *Proc. Natl Acad. Sci. USA* **82**, 3499–3503 (1985).
22. Francel, P.C. *et al.* Neurochemical characteristics of a novel dorsal root ganglion X neuroblastoma hybrid cell line, F-11. *J. Neurochem.* **48**, 1624–1631 (1987).
23. Fan, S.F., Shen, K.F., Scheideler, M.A. & Crain, S.M. F11 neuroblastoma x DRG neuron hybrid cells express inhibitory mu- and delta-opioid receptors which increase voltage-dependent K+ currents upon activation. *Brain Res.* **590**, 329–333 (1992).
24. Zanner, R., Hapfelmeier, G., Gratzl, M. & Prinz, C. Intracellular signal transduction during gastrin-induced histamine secretion in rat gastric ECL cells. *Am. J. Physiol. Cell Physiol.* **282**, C374–C382 (2002).
25. Simasko, S.M., Boyadjieva, N., De, A. & Sarkar, D.K. Effect of ethanol on calcium regulation in rat fetal hypothalamic cells in culture. *Brain Res.* **824**, 89–96 (1999).
26. Burgess, G.M., Mullaney, I., McNeill, M., Dunn, P.M. & Rang, H.P. Second messengers involved in the mechanism of action of bradykinin in sensory neurons in culture. *J. Neurosci.* **9**, 3314–3325 (1989).
27. Tsien, R.W., Lipscombe, D., Madison, D.V., Bley, K.R. & Fox, A.P. Multiple types of neuronal calcium channels and their selective modulation. *Trends Neurosci.* **11**, 431–438 (1988).
28. Davare, M.A., Dong, F., Rubin, C.S. & Hell, J.W. The A-kinase anchor protein MAP2B and cAMP-dependent protein kinase are associated with class C L-type calcium channels in neurons. *J. Biol. Chem.* **274**, 30280–30287 (1999).
29. Hell, J.W., Yokoyama, C.T., Breeze, L.J., Chavkin, C. & Catterall, W.A. Phosphorylation of presynaptic and postsynaptic calcium channels by cAMP-dependent protein kinase in hippocampal neurons. *EMBO J.* **14**, 3036–3044 (1995).
30. Wetzel, C.H., Spehr, M. & Hatt, H. Phosphorylation of voltage-gated ion channels in rat olfactory receptor neurons. *Eur. J. Neurosci.* **14**, 1056–1064 (2001).
31. Liebmann, C. *et al.* Dual bradykinin B2 receptor signalling in A431 human epidermoid carcinoma cells: activation of protein kinase C is counteracted by a GS-mediated stimulation of the cyclic AMP pathway. *Biochem. J.* **313**, 109–118 (1996).
32. Marceau, F., Hess, J.F. & Bachvarov, D.R. The B1 receptors for kinins. *Pharmacol. Rev.* **50**, 357–386 (1998).
33. Austin, C.E. *et al.* Stable expression of the human kinin B1 receptor in Chinese hamster ovary cells. Characterization of ligand binding and effector pathways. *J. Biol. Chem.* **272**, 11420–11425 (1997).
34. Vasko, M.R., Campbell, W.B. & Waite, K.J. Prostaglandin E2 enhances bradykinin-stimulated release of neuropeptides from rat sensory neurons in culture. *J. Neurosci.* **14**, 4987–4997 (1994).
35. Evans, A.R., Nicol, G.D. & Vasko, M.R. Differential regulation of evoked peptide release by voltage-sensitive calcium channels in rat sensory neurons. *Brain Res.* **712**, 265–273 (1996).
36. Linhart, O., Obreja, O. & Kress, M. The inflammatory mediators serotonin, prostaglandin E2 and bradykinin evoke calcium influx in rat sensory neurons. *Neuroscience* **118**, 69–74 (2003).
37. Falcone, R.C. *et al.* Characterization of bradykinin receptors in guinea pig gall bladder. *J. Pharmacol. Exp. Ther.* **266**, 1291–1299 (1993).
38. Pesquero, J.B. *et al.* Hypoalgesia and altered inflammatory responses in mice lacking kinin B1 receptors. *Proc. Natl Acad. Sci. USA* **97**, 8140–8145 (2000).
39. Banik, R.K., Kozaki, Y., Sato, J., Gera, L. & Mizumura, K. B2 receptor-mediated enhanced bradykinin sensitivity of rat cutaneous C-fiber nociceptors during persistent inflammation. *J. Neurophysiol.* **86**, 2727–2735 (2001).
40. Wotherspoon, G. & Winter, J. Bradykinin B1 receptor is constitutively expressed in the rat sensory nervous system. *Neurosci. Lett.* **294**, 175–178 (2000).
41. Fox, A. *et al.* Regulation and function of spinal and peripheral neuronal B1 bradykinin receptors in inflammatory mechanical hyperalgesia. *Pain* **104**, 683–691 (2003).
42. Burgess, S.E. *et al.* Time-dependent descending facilitation from the rostral ventromedial medulla maintains, but does not initiate, neuropathic pain. *J. Neurosci.* **22**, 5129–5136 (2002).
43. Kim, S.H. & Chung, J.M. An experimental model for peripheral neuropathy produced by segmental spinal nerve ligation in the rat. *Pain* **50**, 355–363 (1992).
44. Gardell, L.R. *et al.* Sustained morphine exposure induces a spinal dynorphin-dependent enhancement of excitatory transmitter release from primary afferent fibers. *J. Neurosci.* **22**, 6747–6755 (2002).
45. Cloutier, F., de Sousa Buck, H., Ongali, B. & Couture, R. Pharmacologic and autoradiographic evidence for an up-regulation of kinin B(2) receptors in the spinal cord of spontaneously hypertensive rats. *Br. J. Pharmacol.* **135**, 1641–1654 (2002).
46. Botticelli, L.J., Cox, B.M. & Goldstein, A. Immunoreactive dynorphin in mammalian spinal cord and dorsal root ganglia. *Proc. Natl Acad. Sci. USA* **78**, 7783–7786 (1981).
47. Lai, J. *et al.* The cloned murine M1 muscarinic receptor is associated with the hydrolysis of phosphatidylinositols in transfected murine B82 cells. *Life Sci.* **42**, 2489–2502 (1988).
48. Yaksh, T.L. & Rudy, T.A. Chronic catheterization of the spinal subarachnoid space. *Physiol. Behav.* **17**, 1031–1036 (1976).
49. Chaplan, S.R., Bach, F.W., Pogrel, J.W., Chung, J.M. & Yaksh, T.L. Quantitative assessment of tactile allodynia in the rat paw. *J. Neurosci. Methods* **53**, 55–63 (1994).
50. Hargreaves, K., Dubner, R., Brown, F., Flores, C. & Joris, J. A new and sensitive method for measuring thermal nociception in cutaneous hyperalgesia. *Pain* **32**, 77–88 (1988).